

Ya.V. Burak¹, V.T. Adamiv¹, I.M. Teslyuk¹, I.E. Moroz², S.Z. Malynych^{2,3}

What is the True Value of Bulk Band Gap of Lithium Tetraborate Single Crystal?

¹*O.G. Vlokh Institute of Physical Optics, Lviv, Ukraine, adamiv@ifp.lviv.ua*

²*Lviv Polytechnic National University, Lviv, Ukraine,*

³*Hetman Petro Sahaidachnyi National Army Academy, Lviv, Ukraine, s.malynych@gmail.com*

Substantial variances in the bulk band gap of lithium tetraborate single crystal determined from numerous theoretical calculations as well as from experimental measurements give rise to the problem what is the true value of E_g for that crystal. In this review, we analyze in detail all available theoretical and experimental data regarding the bulk band gap published by different authors and suggest that the experimental value of $E_g^{opt} = (7.5 \pm 0.3)$ eV determined from the optical absorption edge is the most appropriate value. This is in good agreement with the band gap $E_g = 7.5$ eV calculated via modified linear combination of atomic orbitals (LCAO) method.

Keywords: lithium tetraborate, band gap, absorption edge, crystal structure.

Received 17 November 2021; Accepted 28 January 2022.

Introduction

Lithium tetraborate $\text{Li}_2\text{B}_4\text{O}_7$ (LTB) single crystals are widely used in optoelectronics and nonlinear optics due to their exceptional properties as listed below. This non-hygroscopic material has low density $\rho = 2.45$ g/cm³ with hardness after Mohs about 6 [1], low dielectric constant ≈ 9 [2], high pyroelectric and piezoelectric coefficients [3], and appreciable electro-optic parameters [4]. Its broad optical transparency range spans from 165 nm to 6000 nm [5]. Along with high magnitudes of photoelastic coefficients LTB single crystals possess high acousto-optic parameter $M_2 = 2.12 \times 10^{-15}$ s³/kg in a particular crystallographic direction [6, 7]. Thus, LTB single crystals are commonly considered as one of the best acousto-optic materials especially for applications in deep-UV spectral range. It was also found that crystalline LTB is a promising nonlinear-optical material for frequency conversion including fourth-harmonic (266 nm or 4.67 eV) and fifth-harmonic (213 nm or 5.83 eV) generation induced by Nd:YAG laser beam [8, 9]. Currently, there is much interest in LTB single crystals for nonlinear optical conversion into the vacuum ultraviolet using sum frequency mixing with femtosecond pulses

[10]. Remarkably, the material is capable to withstand high power density radiation up to 40 GW/cm².

Lithium tetraborate can be synthesized either in crystalline or glassy form via congruent melting of the compound simply by controlling the annealing rate [11]. The growth of 10 mm in diameter LBO single crystal was first reported in 1977 [12]. Present technology allows growing large single crystals 80 \varnothing × 70 – 105 mm and even up to 200 mm in length [13 - 15].

High electromechanical coupling coefficient factor k^2 and low temperature coefficient delay of acoustic waves make LTB an attractive material for bulk acoustic wave (BAW) and surface acoustic wave (SAW) substrate. SAW devices based on LTB are commonly used as an infrared filter [2, 16]. LTB is also known to be a radiation-resistant material and is used as a tissue-equivalent material for radiation TL dosimetry [17]. Availability of the isotopes ⁶Li and ¹⁰B with natural abundance of 7.4 % and 19.8 % respectively along with a large neutron capture cross-section (940 and 3840 barns respectively) invokes utilizing of LTB single crystal for neutron detection [18, 19]. It is also important that crystalline LTB possesses long carrier lifetime that amounts ~ 120 s and ~ 720 s for $\text{Li}_2\text{B}_4\text{O}_7$ (100) (or X-cut $\text{Li}_2\text{B}_4\text{O}_7$) and $\text{Li}_2\text{B}_4\text{O}_7$ (001) (or

Z-cut $\text{Li}_2\text{B}_4\text{O}_7$) respectively [20]. The cryogenic neutron detector comprising two superconducting tunnel junctions on LTB single crystal was used for two-dimensional neutron imaging with high detection efficiency and spatial resolution of a few microns [21]. Neutron detectors on LTB single crystal operating at cryogenic temperature play an important role in the research that concerns fast or ultra-cold neutrons [22]. The flux of solar neutrons was subtracted from solar proton background and γ -ray radiation and recorded utilizing LTB single crystal detector enriched with ^{10}B (97.3 %) and ^{11}B (99.2 %) that was placed aboard the International Space Station [23].

To estimate the minimum wavelength, which can be obtained in such the experiments, precise position of the absorption edge or the width of the bulk band gap is absolutely necessary to deal with. Despite the vast of works devoted to the theoretical calculations of the band gap of LTB as well as experimental studies the appropriate value of E_g is still under discussion. In present review, the attempt to clarify that issue based on the analysis and comparison of available theoretical and experimental data is presented.

I. Theoretical results

The LTB single crystal has tetragonal symmetry with space group $I4_1cd$ and point group $4mm$ [24, 25]. The unit cell of LTB with lattice parameters $a = b = 9.47 \text{ \AA}$ and $c = 10.28 \text{ \AA}$ at room temperature contains 104 atoms (eight formula units) and is formed by interwoven chains of anionic boron-oxygen complexes $(\text{B}_4\text{O}_9)^{6-}$ that in turn are consisted of planar trigonal 2BO_3 and tetrahedral 2BO_4 groups. The cations Li^+ surrounded by distorted LiO_4 tetrahedron are located in the voids between $(\text{B}_4\text{O}_9)^{6-}$ complexes and serves as the charge compensator (Fig. 1). There is much attention to the studies of LTB crystal structure [24 - 28] including coherent neutron powder diffraction technique [29, 30]. Generally, the crystal structure of lithium tetraborate is well studied. In particular, vibrational spectroscopy studies revealed that LTB single crystal undergoes isostructural phase transition at the temperature 235 K [31].

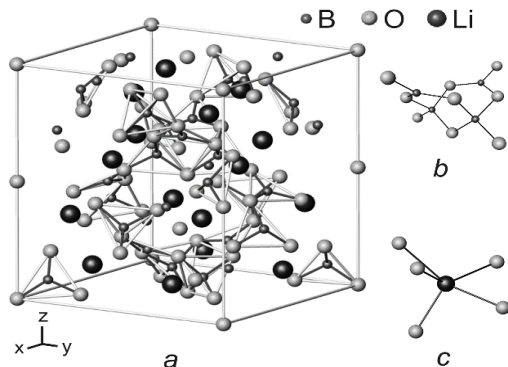


Fig. 1. Crystal structure of $\text{Li}_2\text{B}_4\text{O}_7$: a) isometric projection of lattice unit; b) $(\text{B}_4\text{O}_9)^{6-}$ anionic group structural building block; c) LiO_4 lithium-oxygen tetrahedron.

The results of theoretical calculations of E_g for LTB single crystal performed by different research groups are presented in Table 1. As it is seen from Table 1, the results

are distributed within wide range from 6.18 eV to 18.28 eV [32-36]. This can be explained by the complexity of the unit cell of LTB that put limitations on the employing of traditional one-electron band structure calculation methods such as pseudopotential method, augmented-plane wave method, and even tight-binding approximation (LCAO). So, precise determination of the band gap for LTB single crystal is a challenge, since the value of E_g depends on both atomic set and theoretical method that are chosen for calculations.

Table 1.

Calculated bulk band gap E_g of the lithium tetraborate single crystal.

LCAO	7.5 eV	[32, 33]
PWIPW	9.41 - 8.87 eV	[34]
HF-PW	17.68 - 18.28 eV	[35]
PWIPW	8.94 - 9.75 eV	
B3LYP	8.91 - 9.71 eV	
MSINDO	9.70 eV	
PWGGA	6.80 - 7.40 eV	
PWGG-US	6.31 - 7.34 eV	
PWGGA-PAW	6.27 - 7.31 eV	
PWIPW	9.31 eV	[36]
PW91-PAW	6.18 eV	

As an example, let us demonstrate the initial stage of the band structure calculations for LTB single crystal that was first reported in [32, 33]. The calculations were performed via modified LCAO method. Structural groups BO_3 , BO_4 , LiO_4 and LiO_6 , which on the authors' opinion mainly contribute to the electronic structure of LTB were selected based on crystal chemistry considerations along with phonon spectra. The $2s$ -, $2p_x$ -, $2p_y$ - $2p_z$ -B orbitals and $2s$ -Li orbital were taken into account to construct a secular equation based on Bloch functions for all structural fragments BO_3 , BO_4 , LiO_4 and LiO_6 . Modification of LCAO method relies on a correction of the results accounting the optical functions obtained from fundamental absorption spectrum. Thus, the band structure of LTB that encompasses three coordination spheres was calculated and corrected according to the optical functions to achieve full quantitative agreement. The bulk band gap E_g of LTB single crystal determined in such a way is 7.5 eV.

Wide scattering of the theoretically calculated E_g values that depends on the initial parameters and methods being employed has been clearly demonstrated [34 - 36]. After a closer look at the Table 1 one can see that the band gap $E_g = 17.68 - 18.28 \text{ eV}$ calculated via Hartree-Fock method with Perdew-Wang correlation functional (HF-PW) substantially differs from other results. Let us discard that value, then the rest can be distributed into two groups. The first one is based on Perdew-Wang generalized gradient (PWGG) method and its modifications such as Perdew-Wang with correlation functional based on generalized gradient approximation (PWGGA), PWGG with ultrasoft pseudopotential (PWGG-US), PWGG with

projector augmented-wave (PWGGA-PAW) [35], and Perdew-Wang density functional with projector augmented-wave method (PW91-PAW) [36]. The band gap calculated within mentioned methods is in the range 6.18 - 7.40 eV for LTB single crystal. Recent calculations using linear combination of atomic orbitals (LCAO) method with local density approximation (LDA) based exchange-correlation potential and full potential linearized augmented plane wave (FP-LAPW) method have shown a direct band gap of 5.84 eV and 6.48 eV at Γ point of Brillouin zone respectively [37].

The second group is represented by Hartree-Fock density functional theory or HF-DFT – hybrid approach (PWIPW) [34 - 36], Lee-Yang-Parr correlation functional (B3LYP) [35], and semiempirical molecular method (MSINDO) [35]. The band gap in the second group amounts 8.87 - 9.75 eV. The difference in E_g in that case is caused by the use of two different basis sets for Li, B and O elements. In order to distinguish two different values of the band gap of LTB for the same transition $M \rightarrow \Gamma$ in the Brillouin zone a concept of the minimal transition energy (MT) and minimal vertical transition energy (MVT) was introduced [35, 36]. Probably, the authors meant that MT energy E_T^{min} $E_T^{min} = (6.9 \pm 0.7)$ eV in the range 6.18 - 7.40 eV corresponds to the indirect interband transition, while MVT energy $\Delta E = (9.25 \pm 0.5)$ eV (8.87 - 9.75 eV range) corresponds to the lowest vertical or interband transition for LTB. However, no direct comments on that matter are presented in [35, 36] moreover, the authors used different notations for their results that makes such treatment questionable. Santos *et al.* have found band gap value 9.2 eV using density functional theory-based FP-LAPW method with exchange-correlation potential and assigned it to indirect $X \rightarrow \Gamma$ transition in Brillouin zone [38].

II. Experimental results

One can expect that experimental measurements will shed the light on the problem of the band gap determination for LTB and will indicate on the correct theoretical E_g . However, it occurred that experimental data determined by different researchers also differs, but at the same time can be distributed into two groups, namely 7.43 - 7.76 eV [5, 39, 40] and 9.8 - 10.1 eV [5, 41, 42] (see Table 2). That fact substantially complicates the correct interpretation of the band gap of LTB and requires detail analysis.

Table 2.

Experimental E_g of LTB single crystal as determined from the absorption edge.

7.43 eV (167 nm)	[39]
7.76 eV (160 nm)	[40]
(100) E [100] 10.1 eV	[41, 42]
(100) E [010] 9.0 eV	
(110) E [011] 9.8 eV	
(110) E [010] 9.8 eV	
7.52 eV (165 nm)	[5]

In most cases experimental E_g for LTB single crystal was determined from the absorption edge by measuring the transmission spectra [5, 39, 40]. Studies on the optical transmission range of LTB that spans from 165 nm to 6000 nm were first reported as early as in 1986 [5]. The authors did not mention the width of the band gap, but the absorption edge at 165 nm allows to estimate it as 7.52 eV. Experimental studies of both absorption and reflection spectra of LTB single crystals performed by the same authors in VUV spectral range revealed that the long-wavelength peak of the fundamental absorption closest to the absorption edge is centered at 133 nm (9.33 eV). To detect the potential influence of the local disorder of the LTB crystal lattice optical studies of the absorption edge were performed for single crystal as well as for borate glass (Fig. 2). The spectra of LTB samples were recorded by UV-Vis Specord-M40 and McPherson VUV 2000 spectrophotometers at ambient temperature; VUV spectra were acquired in purified nitrogen atmosphere.

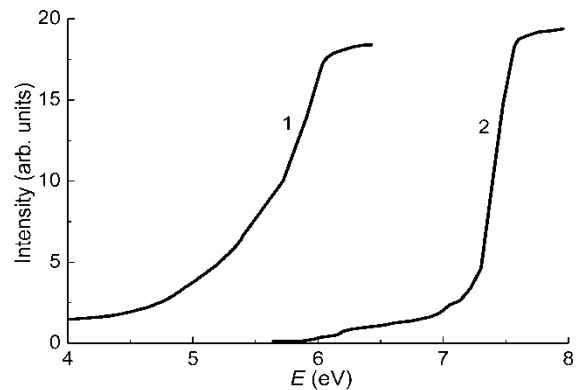


Fig. 2. Intrinsic absorption edge of $\text{Li}_2\text{B}_4\text{O}_7$: (1) glass sample, (2) single crystal.

Glass sample and LTB single crystal with (100) orientation was prepared $10 \times 10 \times 1$ mm in size. As it is seen in Fig. 2 spectral position of the absorption edge for the single crystal and LTB glass substantially differs. It is worth noting that the shoulder at 5.9 - 7.2 eV in the spectrum of LTB single crystal is somewhat similar to that of the glass sample, although it may arise due to non-controlled dopants and/or crystal lattice defects.

The absorption spectrum of LTB glass is typical for glassy samples exhibiting indistinct absorption edge. Since there is no long-range order in the structure of glass, it is expected that band theory cannot be applied directly due to the lack of translational symmetry. To describe electronic structure of disordered media e.g., glass one can use universal characteristics of electronic states, namely electron energy density distribution. In that case, the long-wavelength shift of the absorption edge of the glass in comparison with the single crystals can be explained by blurring of the boundary of the electron density of states. Note that the energy band model is still valid for the glass taking into account that direct interband transitions are forbidden, while only indirect transitions accompanying by phonons and excitons occur. Those indirect optical transitions are considered in detail elsewhere [43].

Boron oxide $(\text{B}_4\text{O}_9)^{6-}$ complex comprising two BO_4

borate groups and two BO_3 ones forms a basis of LTB (Fig. 1b) [24, 30]. It was convincingly shown that the top of valence band of LTB originates from BO_4 tetrahedron, while the bottom of conduction band originates from triangular BO_3 group [32 - 36]. It is naturally to assume that basic structural units of LTB single crystal represented by mentioned boron oxide groups play a key role in the electron density distribution in LTB glass shaping its optical absorption. Thus, the shoulder at 5.9 - 7.2 eV in the absorption spectrum of LTB single crystal may be caused by the translation symmetry violation in crystal lattice akin to what occurs in glass. The fact that structural distortions, in particular at the interface of LTB single crystals, do affect the electron levels in atoms was clearly demonstrated by Wooten et al. [41, 44]. Volume distortions may be represented by long-range order violation such as substitution of tetraborate groups with triborate ones that is typical for LTB glass [45]. Some uncontrolled dopants and excitons discovered by Ogorodnikov may also contribute to the absorption spectrum shoulder [46]. Summarizing the above discussion on the experimental studies of the optical absorption edge one can conclude that the energy of photons absorbed by LTB single crystal is about 7.5 ± 0.3 eV [5, 39, 40]. Thus, the optical band gap of LTB single crystal is accepted as $E_g^{opt} = 7.5 \pm 0.3$ eV. Ambiguity in the experimental determination of LTB band gap was also mentioned in [38].

Quite other values of E_g were obtained from the studies of electronic structure of LTB single crystal employing a combination of angle-resolved photoemission and angle-resolved inverse photoemission spectroscopy [41, 42]. The quality and purity of the samples' surface was among the main concerns in those studies. Cleaning procedure includes resistive heating and combination of sputtering and subsequent annealing. Isolated point defects that amount 2...5 ppm in total do not substantially affect the LTB crystal properties. The measurements were performed in ultra-high vacuum chamber. Synchrotron radiation with photon energy of 56 eV incident at the angle of 45° was used for photoemission studies. Details of the experiment can be found elsewhere [41, 42]. Fig. 3 depicts the intensity of combined photoemission and inverse photoemission as a function of binding energy $E - E_F$, where E_F is the Fermi level.

The direct band gap E_g in mentioned works was defined as the distance between the main maxima of the electron density of states for both valence band and conduction band (see Fig. 3) [41]. Two different values of band gap were found: i) the direct band gap obtained from combined photoemission and inverse photoemission

studies of LTB (100) single crystal is 10.1 ± 0.5 eV and 8.9 ± 0.5 eV with electrical component E of the plane-polarized incident light aligned along [011] and [010] directions respectively; ii) for LTB (110) the direct band gap is 9.8 ± 0.5 eV in both [001] and [110] directions.

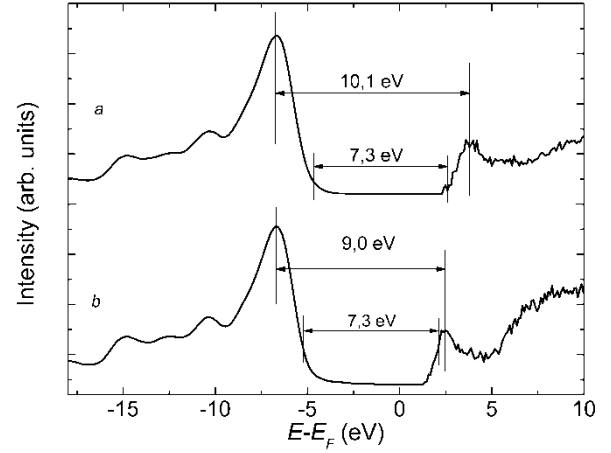


Fig. 3. Combined experimental photoemission and inverse photoemission data for $\text{Li}_2\text{B}_4\text{O}_7$ (100), with electrical component E of the incident electromagnetic wave oriented along (a) [011] and (b) [010], E_F is the Fermi level. The Figure is partially adapted from [41].

It is seen in Fig. 3 that the valence band of LTB consists of several sub-bands that exhibit almost Gaussian distribution of the electron density with the first band being the most intensive. Conduction band has a profound maximum. So, according to [41, 42] the energy interval of 8.9 - 10.1 eV between those two Gaussian distributions of the density of states is considered as the band gap (Fig. 3). It means that photons possessing energy within mentioned range provide transportation of the electrons from valence band to conduction one resulting in the increase of charge carriers – holes in valence band and electrons in conduction band. That gives us a hint to pay attention on the studies of refractive index dispersion employing prism made of LTB single crystal [40, 41]. Therefore, we have decided to use approximation of the refractive index dispersion presented in [40, 47] in the form of Sellmeier equation for the energy range 0.5 - 20 eV. The expressions of Sellmeier equation presented in [40] and [47] are quite similar, but the studies in [40] were performed in 184.9 - 2325.4 nm (6.7 - 0.5 eV) spectral range, while in [47] within 350 - 650 nm (3.5 - 1.9 eV) range. Sellmeier equation in mentioned works is expressed as follows (E in eV)

$$n_0^2 = 2.5643 + \frac{0.012337E^2}{1.5407 - 0.013103E^2} - \frac{0.02934}{E^2}, \quad [40] \quad (1)$$

$$n_0^2 = 2.0424 + \frac{0.5407(1241.25)^2}{1241.25^2 - 133^2E^2} + \frac{2.8910(1241.25)^2}{1241.25^2 - 7407^2E^2}, \quad [47] \quad (2)$$

Here we present Sellmeier equation only for ordinary ray with refractive index n_o . Fig. 4 depicts graphical

solution to equations (1) and (2) presented as a dependence $n_o^2 = f(E)$. Refractive index changes its sign

at photon energy that corresponds to the condition when the denominator in (1) and (2) equals to zero.

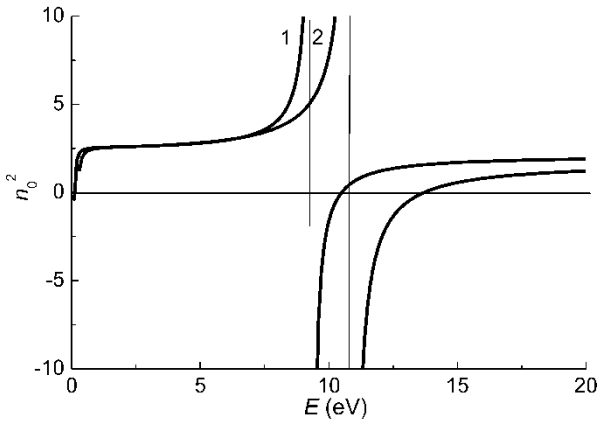


Fig. 4. The plots n_0^2 vs. energy (eV) for the Sellmeier equation (1) and (2).

It is seen in Fig. 4 that refractive index n_o becomes complex at photon energy $E_1 = 9.33$ eV and $E_2 = 10.8$ eV for Eq. (1) and (2) respectively. The solution to Sellmeier equation for an extraordinary ray yield photon energy that corresponds to complex refractive index as $E_1 = 9.33$ eV and $E_2 = 10.9$ eV. The values of energy found from Sellmeier equation are in good agreement with those obtained by combination of angle-resolved photoemission and angle-resolved inverse photoemission spectroscopy $E = 9.8$ eV and 10.1 eV [41, 42]. The energy $E = 10.1 \pm 0.8$ eV is considered in [41, 42] as the band gap of LTB single crystal. On the other hand, incident photons with the energy $9.33 - 10.9$ eV result in the increase of the concentration of electrons in conductive band and holes in valence band i.e., the LTB single crystal changes its state from dielectric to conductive one with complex refractive index

$\tilde{n} = n(1 + \chi)$. Therefore, we suggest to treat the energy $E_n^{ix} = 10.1 \pm 0.8$ eV as one that corresponds to the emerging of intrinsic photoconductivity in LTB single crystal. It is worth noting here that similar ambiguity in the determination of the band gap is observed for lithium niobate single crystal [48].

Conclusions

Based on the comparative analysis of theoretical and experimental studies on electronic structure of lithium tetraborate single crystal presented above, one can conclude there is no unambiguous treatment of the bulk band gap for that material. The conclusion stems from the fact that all mentioned theoretical and experimental data

are clearly distributed into two groups with the difference in energy exceeding 2 eV. The data in the first group are within $6.18 - 7.40$ eV range (theory) and $7.43 - 7.76$ eV that yields $E_g = (6.9 \pm 0.7)$ eV and $E_g = (7.5 \pm 0.3)$ eV respectively. The second group is represented by $E = 8.87 - 9.75$ eV (theory) and $E = 9.8 - 10.1$ eV (experiment) with $E_g = (9.3 \pm 0.5)$ eV and $E_g = (10.1 \pm 0.5)$ eV respectively. Since the experimental results are more realistic, we suggest to consider $E_g^{opt} = (7.5 \pm 0.3)$ eV as the minimum interband transition energy and $E_n^{ix} = (10.1 \pm 0.5)$ eV as the energy of direct vertical interband transition. In other words, E_g^{opt} corresponds to the formation of the absorption edge, while E_n^{ix} is photon energy corresponding to the complex refractive index $\tilde{n} = n(1 + \chi)$ of LTB single crystal caused by high electron concentration in the conductive band. So, E_g^{opt} can be considered as bulk band gap of the LTB single crystals in traditional meaning.

The existence of two distinct values E_g^{opt} and E_n^{ix} of the band gap of LTB single crystal can be explained by the features in electron density distribution in both valence and conductive bands, which is similar to that for LTB glass. Variance in theoretical estimation of the bulk band gap of LTB single crystal is due to the complex character of the crystal structure. The shoulder at $(5.9 - 7.2)$ eV in the absorption spectrum of LTB single crystal is associated with lattice defects, in particular with long-range order violation, uncontrolled dopants and, possibly, with contribution of the indirect interband transitions. It is worth noting that theoretical estimation of LTB single crystal bulk band gap $E_g = 7.5$ eV calculated via modified LCAO method [32, 33] is almost equal to the experimental one $E_g^{opt} = (7.5 \pm 0.3)$ eV. The results obtained by PWGGA ($6.80 - 7.40$) eV, PWGG-US ($6.31 - 7.34$) eV and PWGGA-PAW ($6.27 - 7.31$) eV methods [36] partially overlap with the shoulder in the absorption spectrum of LTB single crystal and are quite close to the optical band gap.

Funding

Ministry of Education and Science of Ukraine (grant 0119U100357).

Burak Ya.V. - Doctor of Science Leading scientist;
Adamiv V.T. – Doctor of Science Head of the Department of Optical Materials Science;
Teslyuk I.M. – Research Associate;
Moroz I.E. – PhD Associate Professor, Department of Physics;
Malynych S.Z. - Doctor of Science Professor, Department of Electromechanics and Electronics.

- [1] M. Natarajan, R. Faggini, I. Brown, Cryst. Struct. Comm. 8, 367 (1979).
- [2] K. Fukuta, J. Ushizawa, H. Suzuki, J. Ebata, S. Matsumura, Jpn. J. Appl. Phys. 22, 140 (1983); <https://iopscience.iop.org/article/10.7567/JJAPS.22S2.140>.
- [3] Bhalla, E. Cross, R. Whatmore, Jpn. J. Appl. Phys. 24, 727 (1985); <https://iopscience.iop.org/article/10.7567/JJAPS.24S2.727>.
- [4] V. D. Antsygin, V. A. Gusev, A. M. Yurkin, Avtometriya, N3, 16 (1996).
- [5] O. Antonyak, Ya. Burak, I. Lyseiko, M. Pidzyrajlo, Z. Khapko, Opt. Spectrosc. 61, 550 (1986).

- [6] B.G. Mytsyk, A.S. Andrushchak, D.M. Vynnyk, N.M. Demyanyshyn, Ya.P. Kost, A.V. Kityk, *Optics and Lasers in Engineering*, 127, 105991 (2020); <https://doi.org/10.1016/j.optlaseng.2019.105991>.
- [7] O. Krupych, O. Mys, T. Kryvyy, V. Adamiv, Ya. Burak, R. Vlokh, *Appl. Opt.* 55, 10457 (2016); <https://doi.org/10.1364/AO.55.010457>.
- [8] R. Komatsu *et al.*, *Appl. Phys. Lett.* 70, 3492 (1997); <https://doi.org/10.1063/1.119210>.
- [9] G.C. Bhar, A.K. Chaudhary, P. Kumbhakar, A.M. Rudra, *J. Phys. D: Appl. Phys.* 34, 360 (2001); <https://iopscience.iop.org/article/10.1088/0022-3727/34/3/319>.
- [10] V. Petrov, F. Rotermund, F. Noack, *J. Appl. Phys.* 84, 5877 (1998); <https://doi.org/10.1063/1.368904>.
- [11] B. Sastry, F. Hummel, *J. Am. Ceram. Soc.* 41, 7 (1958); <https://doi.org/10.1111/j.1151-2916.1958.tb13496.x>.
- [12] J. Garrett, M. Iyer, J. Greedan, *J. Cryst. Growth* 41, 225 (1977); [https://doi.org/10.1016/0022-0248\(77\)90049-5](https://doi.org/10.1016/0022-0248(77)90049-5).
- [13] R. Komatsu, T. Sugihara, S. Uda, *Jpn. J. Appl. Phys.* 33, 5533 (1994); <https://iopscience.iop.org/article/10.1143/JJAP.33.5533>.
- [14] J. Tsutsui, Y. Ino, N. Sanguttuvan, M. Ishii, *J. Cryst. Growth* 211, 271 (2000); [https://doi.org/10.1016/S0022-0248\(99\)00860-X](https://doi.org/10.1016/S0022-0248(99)00860-X).
- [15] J. Xu, S. Fan, B. Lu, *J. Cryst. Growth* 264, 260 (2004); <https://doi.org/10.1016/j.jcrysgro.2003.12.040>.
- [16] M. Takeuchi, H. Odagawa, M. Tanaka, K. Yamanouchi, *Jap. J. Appl. Phys.* 36, 3091 (1997); <https://iopscience.iop.org/article/10.1143/JJAP.36.3091>.
- [17] C. Furetta, P. Weng, *Operation Thermoluminescent Dosimetry* (World Scientific, London, 1998).
- [18] Ya.V. Burak, B.V. Padlyak, V.M. Shevel, *Nucl. Instr. Meth. In Phys. Res. B* 191, 633 (2002); [https://doi.org/10.1016/S0168-583X\(02\)00624-9](https://doi.org/10.1016/S0168-583X(02)00624-9).
- [19] Sangeeta, K. Chennakesavulu, D.G. Desai, S.C. Sabharwal, M. Alex, M.B. Chodgaonkar, *Nucl. Instr. Meth. Phys. Res. A* 571, 699 (2007); <https://doi.org/10.1016/j.nima.2006.10.401>.
- [20] Z. G. Marzouk, A. Dhingra, Y. Burak, V. Adamiv, I. Teslyuk, P. A. Dowben, *Materials Letters*, 97, 129978 (2021); <https://doi.org/10.1016/j.matlet.2021.129978>.
- [21] T. Nakamura, M. Katagiri M, Y.E. Chen, M. Ukibe M, M. Ohkubo, *Nucl. Instr. Meth. Phys. Res. A* 559, 766 (2006); <https://doi.org/10.1016/j.nima.2005.12.131>.
- [22] M. Katagiri, *Nucl. Instr. Meth. Phys. Res. A* 559, 742 (2006); <https://doi.org/10.1016/j.nima.2005.12.124>.
- [23] N. Benker *et al.*, *Rad. Meas.* 129, 106190 (2019); <https://doi.org/10.1016/j.radmeas.2019.106190>.
- [24] J. Krogh-Moe, *Acta Cryst.* 15, 190 (1962); <https://doi.org/10.1107/S0365110X6200050X>.
- [25] J. Krogh-Moe, *Acta Cryst. B* 24, 179 (1968); <https://doi.org/10.1107/S0567740868001913>.
- [26] W. H. Zachariasen, *Acta Cryst.* 17, 749 (1964); <https://doi.org/10.1107/S0365110X64001839>.
- [27] V. T. Adamiv, Ya. V. Burak, I. M. Teslyuk, *J. Alloy. Compd.* 475, 869 (2009); <https://doi.org/10.1016/j.jallcom.2008.08.017>.
- [28] S. Radaev, L. Muradyan, L. Malakhova, Ya. Burak, V. Simonov, *Crystallogr. Reports* 34, 1400 (1989).
- [29] Senyshyn *et al.*, *J. Appl. Phys.* 108, 093524 (2010); <https://doi.org/10.1063/1.3504244>.
- [30] Senyshyn *et al.*, *J. Phys. D: Appl. Phys.* 45, 175305 (2012); <https://doi.org/10.1088/0022-3727/45/17/175305>.
- [31] Ya. V. Burak, I. E. Moroz, *Physics and Chemistry of Glasses* 44(3), 241 (2003).
- [32] Ya. Burak, Ya. Dovgyi, I. Kityk, *Phys. Solid State* 31, 275 (1988).
- [33] V. Adamiv *et al.*, *Opt. Mater.* 8, 207 (1997); [https://doi.org/10.1016/S0925-3467\(97\)00017-7](https://doi.org/10.1016/S0925-3467(97)00017-7).
- [34] V. Maslyuk, M. Islam, Th. Bredow, *Phys. Rev. B* 72, 125101-8 (2005); <https://doi.org/10.1103/PhysRevB.72.125101>.
- [35] M. Islam, V. Maslyuk, T. Bredow, C. Minot, *J. Phys. Chem. B.* 109, 13597 (2005); <https://doi.org/10.1021/jp044715q>.
- [36] M. Islam, T. Bredow, C. Minot, *J. Phys. Chem. B* 110, 117518 (2006); <https://doi.org/10.1021/jp061785j>.
- [37] P. K Jangid, G. Arora, D. Mali, P K Joshi, K. Kumar, B L. Ahuja, *Journal of Physics: Conference Series* 1504, 012017 (2020); <https://doi.org/10.1088/1742-6596/1504/1/012017>.
- [38] Santos, A.F. Lima, M.V. Lalic, *Computational Materials Science* 95, 271 (2014); <http://dx.doi.org/10.1016/j.commatsci.2014.07.038>.
- [39] Podgorska, S. Kaczmarek, W. Drozdowski, M. Berkowski, A. Worczytnowicz, *Acta Phys. Pol. A* 107, 507 (2005); <https://doi.org/10.12693/APhysPolA.107.507>.
- [40] T. Sugawara, R. Komatsu, S. Uda, *Sol. State Commun.* 107, 233 (1998); [https://doi.org/10.1016/S0038-1098\(98\)00190-2](https://doi.org/10.1016/S0038-1098(98)00190-2).
- [41] D. Wooten *et al.*, *Eur. Phys. J. Appl. Phys.* 52, 31601-p7 (2010); <https://doi.org/10.1051/epjap/2010160>.
- [42] V. Adamiv *et al.*, *Materials* 3, 4550 (2010); <https://doi.org/10.3390/ma3094550>.
- [43] Y. Moustafa, A. Hassan, G. El-Damrawi, N. Yevtushenko, *J. Non-Cryst. Solids* 194, 34 (1996); [https://doi.org/10.1016/0022-3093\(95\)00465-3](https://doi.org/10.1016/0022-3093(95)00465-3).
- [44] Wooten *et al.*, *Physica B* 405, 461 (2010); <https://doi.org/10.1016/j.physb.2009.08.312>.
- [45] B. Padlyak *et al.*, *Mat.Sci.-Poland* 30, 264 (2012); <https://doi.org/10.2478/s13536-012-0032-1>.
- [46] Ogorodnikov *et al.*, *Phys. Solid State* 42, 464 (2000); <https://doi.org/10.1134/1.1131232>.
- [47] Ya. Burak, G. HycKaylo, M. Pidzyraylo, I. Stephanskiy, *Ukr. J. Phys.* 32, 1509 (1987).
- [48] C. Thierfelder, S. Sanna, A. Schindlmayr, W. G. Schmidt, *Phys. Status Solidi C* 7(2), 362 (2010); <https://doi.org/10.1002/pssc.200982473>.

Я.В. Бурак¹, В.Т. Адамів¹, І.М. Теслюк¹, І.Є. Мороз², С.З. Малинич^{2,3}

Якою є справжня ширина забороненої зони монокристалу тетраборату літію?

¹Інститут фізичної оптики ім. О.Г. Влоха, Львів, Україна, adamiv@ifp.lviv.ua.

²Національний університет «Львівська політехніка», Львів, Україна

³Національна академія сухопутних військ імені гетьмана Петра Сагайдачного, Львів, Україна, s.malynych@gmail.com

Суттєві відмінності значень ширини забороненої зони монокристалів тетраборату літію, отримані із численних теоретичних розрахунків та експериментальних вимірювань піднімають питання: якою ж є дійсна ширина забороненої зони цього кристалу? У цьому огляді ми детально аналізуємо всі можливі теоретичні та експериментальні дані стосовно ширини забороненої зони масивних монокристалів, опубліковані різними авторами, а також пропонуємо, що експериментальне значення $E_g^{opt} = (7.5 \pm 0.3)$ eV, отримане з вимірювань крайового поглинання, є найбільш прийнятним. Це значення добре узгоджується з шириною забороненої зони $E_g = 7.5$ eV, обчисленої з використанням модифікованого методу лінійної комбінації атомних орбіталей (ЛКАО).

Ключові слова: тетраборат літію, ширина забороненої зони, край поглинання, кристалічна структура.